# Solution Synthesis of Alkyl- and Alkyl/Alkoxy-Capped Silicon Nanoparticles via Oxidation of $Mg_2Si$

Katherine A. Pettigrew, Qi Liu, Philip P. Power, and Susan M. Kauzlarich*

*Department of Chemistry, One Shields Ave, University of California, Davis, California 95616*

*Received May 23, 2003. Revised Manuscript Received July 30, 2003*

Alkyl-capped and alkyl/alkoxy-capped silicon nanocrystals have been prepared by the oxidation of magnesium silicide with bromine. High-resolution transmission electron microscopy confirmed the crystalline nature of the nanoparticles and provided an average diameter of 4.5 (2.0) nm for the alkyl-capped and for the alkyl/alkoxy-capped nanoparticles. Energy-dispersive X-ray spectroscopy showed that the nanoparticles are composed of silicon, with no evidence of unreacted bromine. FTIR spectra were consistent with alkyl- and alkyl/alkoxy-capped surfaces. Fluorescence spectroscopy indicated strong ultraviolet-blue photoluminescence, which was attributed to both quantum confinement and surface termination. These nanoparticles displayed long-term stability and no degradation of the photoluminescence was observed for a period of 1 year.

## Introduction

It is well-known that the size of a semiconductor nanocluster affects the energy of the band gap.[1−3] Investigation of the synthesis of silicon nanoparticles by solution routes[4−13] has been an active area of research since it was first suggested that the visible luminescence seen in porous silicon could result from quantum confinement.[14] Several research groups have demonstrated the fluorescence of silicon nanoparticles in the blue, green, yellow, and red regions of the spectrum, which is consistent with quantum confinement.[11,15,16] In addition, there is evidence that silicon shows many of the attributes of conventional II−IV nanoparticles, such as short lifetimes, high quantum yields, and stimulated emission, useful properties for tags for biologically sensitive materials, and applications in optoelectronics.[10,17−24] However, there is no experimental agreement on the relationship between the size of silicon nanoparticles and the emission energies.[5,25,26] It is clear that each synthetic method produces different materials with different shapes and surfaces. It has been recognized recently that surface termination, as well as possible surface reconstruction of silicon nanoclusters, can affect the photophysics of these species.[25−33]

Various routes for the production of well-characterized, surface-capped Si nanoparticles have been explored.[7,8,12,13,15,34−37] In particular, the use of metal

* To whom correspondence should be addressed. E-mail: smkauzlarich@ucdavis.edu.

(1) Brus, L. *J. Phys. Chem.* **1986**, *90*, 2555−2560.
(2) Murray, C. B.; Norris, D. J.; Bawendi, M. G. *J. Am. Chem. Soc.* **1993**, *115*, 8706−8715.
(3) Alivisatos, A. P. *J. Phys. Chem.* **1996**, *100*, 13226−13239.
(4) Heath, J. R. *Science* **1992**, *258*, 1131−1133.
(5) Wilcoxon, J. P.; Samara, G. A.; Provencio, P. N. *Phys. Rev. B: Condens. Matter* **1999**, *60*, 2704−2714.
(6) Wilcoxon, J. P.; Samara, G. A. *Appl. Phys. Lett.* **1999**, *74*, 3164−3166.
(7) Yang, C. S.; Bley, R. A.; Kauzlarich, S. M.; Lee, H. W. H.; Delgado, G. R. *J. Am. Chem. Soc.* **1999**, *121*, 5191−5195.
(8) Yang, C. S.; Kauzlarich, S. M.; Wang, Y. C.; Lee, H. W. H. *J. Clust. Sci.* **2000**, *11*, 423−431.
(9) Holmes, J. D.; Ziegler, K. J.; Doty, R. C.; Pell, L. E.; Johnston, K. P.; Korgel, B. A. *J. Am. Chem. Soc.* **2001**, *123*, 3743−3748.
(10) Harwell, D. E. Synthesis of silicon nanoparticles and metal-centered silicon nanoparticles and applications thereof. PCT Int. Appl., 2001 (CODEN: PIXXD2 WO 0114250 A2 20010301 CAN 134:19 5277 AN 2001:152587 CAPLUS); UH Reference No. 00227, University of Hawaii, 2002.
(11) English, D. S.; Pell, L. E.; Yu, Z.; Barbara, P. F.; Korgel, B. A. *Nano Lett.* **2002**, *2*, 681−685.
(12) Baldwin, R. K.; Pettigrew, K. A.; Garno, J. C.; Power, P. P.; Liu, G. Y.; Kauzlarich, S. M. *J. Am. Chem. Soc.* **2002**, *124*, 1150−1151.
(13) Baldwin, R. K.; Pettigrew, K. A.; Ratai, E.; Augustin, M. P.; Kauzlarich, S. M. *Chem. Commun.* **2002**, 1822−1823.
(14) Canham, L. T. *Appl. Phys. Lett.* **1990**, *57*, 1046−1048.
(15) Lee, H. W. H.; Thielen, P. A.; Delgado, G. R.; Kauzlarich, S. M.; Yang, C.-S.; Taylor, B. R. *Crit. Rev. Opt. Sci. Technol.* **2000**, *CR77* (Novel Materials and Crystal Growth Techniques for Nonlinear Optical Devices), 147−164.
(16) Belomoin, G.; Therrien, J.; Smith, A.; Rao, S.; Twesten, R.; Chaieb, S.; Nayfeh, M. H.; Wagner, L.; Mitas, L. *Appl. Phys. Lett.* **2002**, *80*, 841−843.
(17) Nozaki, S.; Sato, S.; Ono, H.; Morisaki, H. *Mater. Res. Soc. Symp. Proc.* **1994**, *351*, 399.
(18) Brus, L. *J. Phys. Chem.* **1994**, *98*, 3575−3581.
(19) Shah, A.; Torres, P.; Tscharner, R.; Wyrsch, N.; Keppner, H. *Science* **1999**, *285*, 692−698.
(20) Nayfeh, M. H.; Akcakir, O.; Belomoin, G.; Barry, N.; Therrien, J.; Gratton, E. *Appl. Phys. Lett.* **2000**, *77*, 4086−4088.
(21) Therrien, J.; Belomoin, G.; Nayfeh, M. *Appl. Phys. Lett.* **2000**, *77*, 1668−1670.
(22) Nayfeh, M. H.; Barry, N.; Therrien, J.; Akcakir, O.; Gratton, E.; Belomoin, G. *Appl. Phys. Lett.* **2001**, *78*, 1131−1133.
(23) Nayfeh, M. H.; Rao, S.; Barry, N.; Therrien, J.; Belomoin, G.; Smith, A.; Chaieb, S. *Appl. Phys. Lett.* **2002**, *80*, 121−123.
(24) Roland, C.; Meunier, V.; Larade, B.; Guo, H. *Phys. Rev. B* **2002**, *66*, 035332.
(25) Garoufalis, C. S.; Zdetsis, A. D.; Grimme, S. *Phys. Rev. Lett.* **2001**, *87*, 276402−276404.
(26) Williamson, A. J.; Grossman, J. C.; Hood, R. Q.; Puzder, A.; Galli, G. *Phys. Rev. Lett.* **2002**, *89*, 196803.
(27) Wolkin, M. V.; Jorne, J.; Fauchet, P. M.; Allan, G.; Delerue, C. *Phys. Rev. Lett.* **1999**, *82*, 197−200.
(28) Mitas, L.; Therrien, J.; Twesten, R.; Belomoin, G.; Nayfeh, M. H. *Appl. Phys. Lett.* **2001**, *78*.
(29) Vasiliev, I.; Chelikowsky, J. R.; Martin, R. M. *Phys. Rev. B* **2002**, *65*, 121302(R).
(30) Puzder, A.; Williamson, A. J.; Grossman, J. C.; Galli, G. *Phys. Rev. Lett.* **2002**, *88*, 097401/097401−097404.
(31) Pizzagalli, L.; Galli, G. *Mater. Sci. Eng.* **2002**, *B96*, 86−89.
(32) Puzder, A.; Williamson, A. J.; Grossman, J. C.; Galli, G. *J. Chem. Phys.* **2002**, *117*, 6721−6729.
(33) Puzder, A.; Williamson, A. J.; Grossman, J. C.; Galli, G. *Mater. Sci. Eng.* **2002**, *B96*, 80−85.

10.1021/cm034403k CCC: $25.00 
Published on Web 08/30/2003

silicides has been investigated[38] as precursors to silicon nanoparticles with subsequent surface passivation with organic ligands. The synthesis involves a metathesis reaction of the metal silicide with silicon tetrachloride and subsequent termination with alkyl groups. These nanoparticles were shown to be highly crystalline, faceted nanoparticles with no oxygen termination on the surface.[7,8] They also showed strong UV-blue photoluminescence.[7] Since this synthetic method produced a distribution of sizes, all the visible colors were observable in the fluorescence spectra.[15] Although these nanoparticles were stable and displayed no detectable change after storage for 1 year, desirable reaction traits such as high yields and narrow size distributions have not been forthcoming.

Recently, two new routes have been investigated with the objective of a high-yield synthesis for alkyl-capped silicon nanoparticles. These involve the oxidation of metal silicide[37,39] and the reduction of silicon tetrahalides and other alkylsilicon halides.[12,13] The oxidation route for the solution synthesis of silicon nanoparticles is presented in this paper. It involves the oxidation of magnesium silicide with bromine and subsequent termination of the nanoparticles by means of an alkyllithium reagent. The oxidation route provides a means of controlling the size of the nanoparticles by controlling surface termination with the amount of bromine introduced into the synthesis. This provides a nanoparticle capped with bromine, which is then passivated. Passivation is expected to provide long stability to the nanoparticle.[40,41] The nanoparticles were characterized by transmission electron microscopy (TEM), high-resolution TEM (HRTEM), energy-dispersive X-ray spectroscopy (EDX), Fourier transform infrared spectroscopy (FTIR), UV−vis, and photoluminescence (PL).

## Experimental Procedure

**Chemicals.** All reagents and materials were handled either in a nitrogen-filled drybox (Vacuum Atmospheres HE−493) or on a Schlenk line using standard anaerobic and anhydrous techniques. Magnesium flake (99.9%) was purchased from Strem and silicon (99.999+%) was obtained from Johnson Matthey. Anhydrous *n*-octane (99+%, Aldrich) and anhydrous ethylene glycol dimethyl ether (glyme) (99.5%, Aldrich) were dried by distillation over sodium−potassium alloy in an argon atmosphere. *n*-Butyl alcohol (Aldrich) was dried over sodium. *n*-Butyllithium (*n*-BuLi, 1.6 M in hexane) was obtained from Aldrich and used as supplied. HPLC-grade hexane and water were purchased from Aldrich and used without further purification. All glassware was silanated for 1−2 h with a 2% solution of dichlorodimethylsilane in toluene, rinsed with toluene and hexane, and dried at 120 °C overnight prior to use.

**Synthesis.** Magnesium silicide ($Mg_2Si$) was prepared by heating stoichiometric amounts of magnesium flakes with silicon powder at 750 °C for 3 days in a sealed tantalum tube, enclosed in an evacuated quartz ampule as previously described.[42] The product is a metallic blue powder and it was characterized by X-ray powder diffraction. The diffraction pattern obtained agreed with the calculated pattern for the anti-fluorite structure of $Mg_2Si$.[42]

*Preparation of Silicon Nanoclusters.* Silicon nanoparticles were synthesized by the reaction of finely ground $Mg_2Si$, suspended in dry, degassed octane or glyme, with bromine, which was added through an airtight syringe. A parallel reaction using iodine instead of bromine gave a very low nanoparticle yield and X-ray powder diffraction studies of the final product showed large amounts of unreacted $Mg_2Si$. No further reactions with iodine were pursued and all subsequent reactions were performed with bromine. Bromine was added either at room temperature or when the solvent (glyme) was slightly above its freezing point (−58 °C).

*Synthesis in n-Octane.* Bromine (0.54 mL, 1.68 g, 10.5 mmol) was added through an airtight syringe to $Mg_2Si$ (0.100 g, 1.30 mmol) suspended in octane (100 mL) at room temperature and the mixture was stirred for 2 h, during which time the color changed from deep reddish brown to a light gray-brown. The mixture was heated slowly to reflux and the color disappeared after 30 min of heating. Upon further refluxing for 60 h, the mixture changed to a brownish black suspension, which was then cooled to room temperature. The solvent and any remaining $Br_2$ were removed under reduced pressure.

*Synthesis in Glyme.* Bromine (0.20 mL, 0.62 g, 3.90 mmol) was added through an airtight syringe to $Mg_2Si$ (0.100 g, 1.30 mmol) suspended in glyme (200 mL) with cooling to ca. −50 °C. The mixture was stirred until it reached room temperature, and as the reaction warmed, an orange-white solid formed (determined to be $MgBr_2$ by X-ray powder diffraction). The mixture was refluxed for 19 h, during which time the solution changed from a dark orange/brown color with blue and white/orange precipitates to a dark brown color with some white and some blue precipitates. No characterization of this intermediate was performed.

*Surface Termination of Silicon Nanoclusters.* Freshly distilled *n*-octane (100 mL) was added to the bromine-capped silicon nanoclusters originally synthesized in *n*-octane. These were then terminated with *n*-BuLi (3.26 mL, 5.22 mmol), which was added to the reaction via an airtight syringe at room temperature. The mixture was stirred at room temperature for 2 days, whereupon the solvent was removed under reduced pressure. An aqueous solution of 1 M HCl (100 mL) was added to the reaction flask to dissolve and remove any salts. HPLC-grade hexane (30 mL) was then added to extract the nanoparticles. The mixture was transferred to a separatory funnel and washed with water several times. The collected hexane layer was clear and colorless. The hexane was then removed by air evaporation to yield an oily residue (0.006 g), which contained the nanoparticles. The average diameter of the silicon nanoparticles is 4.9 (2.3) nm (determined from HR-TEM). This oily residue could be re-suspended in hexane for further characterization.

The termination process was slightly different for the nanoparticles prepared in glyme. The reaction flask was cooled to −50 °C and *n*-BuLi (2.50 mL, 4.00 mmol) was added. The mixture was warmed to room temperature and stirred for 1 h during which time a white solid formed. Then *n*-BuOH (4.00 mL) was syringed into the reaction flask. The solution was stirred for 30 min, after which time the solvent was removed under reduced pressure. HPLC-grade hexane (30 mL) was added to extract the nanoparticles along with 1 M HCl aqueous solution (200 mL) to dissolve and remove any salts. This mixture was transferred to a separatory funnel and washed with HPLC-grade water several times. The hexane layer was separated and collected in a vial. The hexane was removed by

(34) Bley, R. A.; Kauzlarich, S. M. *J. Am. Chem. Soc.* **1996**, *118*, 12461−12462.
(35) Bley, R. A.; Kauzlarich, S. M. In *Nanoparticles and Nanostructures Films*; Fendler, J. H., Ed.; Wiley-VCH: Weinheim, 1998; pp 101−118.
(36) Mayeri, D.; Phillips, B. L.; Augustine, M. P.; Kauzlarich, S. M. *Chem. Mater.* **2001**, *13*, 765−770.
(37) Liu, Q.; Kauzlarich, S. M. *Mater. Sci. Eng.* **2002**, *B96*, 72−75.
(38) Kauzlarich, S. M.; Chan, J. Y.; Taylor, B. R. In *Inorganic Materials Synthesis*; Winter, C. H., Hoffman, D. M., Eds.; ACS Symposium Series 727; American Chemical Society: Washington D.C., 1999; pp 15−27.
(39) Pettigrew, K. A.; Power, P. P.; Kauzlarich, S. M. *Mater. Res. Soc. Symp. Proc.* **2003**, *75*, F1.8.1−1.8.6.
(40) Stewart, M. P.; Buriak, J. M. *Comments Inorg. Chem.* **2002**, *23*, 179−203.
(41) Buriak, J. M. *Chem. Rev.* **2002**, *102*, 1271−1308.
(42) Li, G. H.; Gill, H. S.; Varin, R. A. *Metall. Trans. A, Phys. Metall. Mater. Sci.* **1993**, *24A*, 2383−2391.

air evaporation to yield 0.023 g of the nanoparticles as a yellow oil. For this reaction the average diameter of the silicon nanoparticles is 4.8 (2.0) nm (determined from HRTEM). These nanoparticles were then re-suspended in hexane for further characterization.

**Characterization.** X-ray powder diffraction data for the solids were obtained on either an Inel powder diffractometer or by means of a Guinier powder diffraction camera. Data analysis was performed by use of commercial software. An FTIR spectrum of the neat nanoparticles was obtained at room temperature by dropping the hexane colloid on to a KBr plate and allowing the solvent to evaporate. The spectrum was collected on a Mattson Galaxy series FTIR 3000 spectrometer. Photoluminescence spectra of the hexane colloid in a quartz cuvette were obtained with either a Perkin-Elmer LS50B or a FluoroMax-P luminescence spectrophotometer. A blank of pure HPLC-grade hexane was examined before recording each sample. Transmission electron microscopy (TEM) and high-resolution TEM samples were prepared by evaporation of the colloids on holey and continuous carbon-coated 400-mesh electron microscope grids followed by baking in a 120 °C oven for 3 h. The electron microscopes were a Philips CM-200 high-resolution TEM (HRTEM) operating with a 200-keV accelerating voltage at the National Center of Electron Microscopy (NCEM) and a Philips CM-12 TEM operating with a 100-keV accelerating voltage at the University of California, Davis.

## Results and Discussion

**Synthesis.** The nanoparticles were formed according to eqs 1 and 2. The reaction involves the oxidation of magnesium silicide with bromine and the subsequent termination of the $Si_mBr$ product with use of an alkyl lithium reagent.

$$m\mathrm{Mg_2Si} + 2.5m\mathrm{Br_2} \rightarrow \mathrm{Si}_m\mathrm{Br} + 2m\mathrm{MgBr_2} \quad (1)$$

$$\mathrm{Si}_m\mathrm{Br} + n\text{-BuLi} \rightarrow n\text{-BuSi}_m + \mathrm{LiBr} \quad (2)$$

Once the alkyl-capped product was obtained, the solvent was removed under reduced pressure, and hexane was added. The hexane mixture was washed a number of times with acidified water to remove the salt byproducts such as lithium bromide, magnesium bromide, excess *n*-BuLi and other byproducts of the reaction.

The solvents employed in the reaction were octane and 1,2-dimethoxyethane (glyme). Octane was chosen because of its inertness toward bromine. However, glyme has often been the solvent of choice for reactions involving magnesium silicide and other Zintl-salts.[7,8,34,35,37,43−49] Of the two solvents investigated, glyme provided yields that were almost 4 times larger than the corresponding reactions in octane. It is possible that the higher yields are due to an increased amount of impurity in the product. However, TEM and photoluminescent characterization are consistent with an increased yield of capped silicon nanoparticle product.

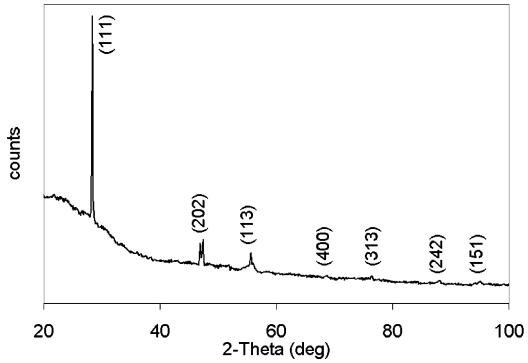


**Figure 1.** Powder XRD pattern for the product formed when excess bromine was refluxed with $Mg_2Si$ in glyme for 48 h. The powder diffraction pattern is indexed as bulk, crystalline silicon.

Since $Mg_2Si$ does not dissolve in any solvent to an appreciable extent, it can be assumed that the reaction is a heterogeneous surface reaction. Consequently, the $Mg_2Si$ was ground to a very fine powder, which promotes the reaction due to higher surface area. The reaction was performed several times in octane according to eq 1, with use of an excess of bromine. The highest yields were obtained by refluxing for 60 h, which ensured complete reaction of magnesium silicide. Unreacted magnesium silicide could be observed with shorter reaction times.

In contrast to the reaction in octane, a black precipitate was obtained after refluxing in glyme for 48 h. No unreacted magnesium silicide powder could be observed in the reaction flask. The nanoparticles present were capped by the addition of *n*-BuLi and separated with use of a hexane/water extraction as described in the Experimental Section. The black precipitate was dried and analyzed by X-ray powder diffraction (Figure 1). The diffraction pattern was indexed as bulk crystalline silicon. Subsequent reactions were performed with shorter reflux times (15−19 h) and limited amounts of bromine. The product from these reactions contain nanoparticles which exhibit crystalline electron-diffraction patterns in the TEM, but do not show powder diffraction patterns by conventional XRD. The products are more fully characterized and discussed below. Bromine was added to the magnesium silicide solvent mixture at −50 °C. The reaction was performed with $m = 4$, that is, a silicon:bromine ratio of 4:1 or $Si_4Br$, to obtain control over the size of the nanoparticles. This ratio was expected to produce a 4-nm-diameter particle. A 4-nm-diameter particle was targeted simply to ease characterization of the product by TEM. The ratio of 4:1 silicon:bromine is expected to produce a 4-nm-diameter particle based on crystal structure, density, and termination of dangling bonds composed of approximately 3600 silicon atoms and 900 surface sites bound to bromine. It was found that by lowering the temperature prior to the addition of bromine, and limiting the amounts of bromine, produced the narrowest size distribution and the highest yields. Taking into account the average size of the nanoparticles and assuming that all the product was nanoparticles, a percentage yield can be calculated. The percentage yield for the reaction performed in octane is 10.9% and for the reaction performed in glyme, 41.8%.

(43) Bley, R. A.; Kauzlarich, S. M. In *Nanoparticles in Solids and Solutions*; Fendler, J. H., Dékány, I., Eds.; Kluwer Academic Press: Dordrecht, The Netherlands, 1996; pp 467−475.
(44) Taylor, B. R.; Kauzlarich, S. M.; Lee, H. W. H.; Delgado, G. R. *Chem. Mater.* **1998**, *10*, 22−24.
(45) Taylor, B. R.; Kauzlarich, S. M.; Delgado, G. R.; Lee, H. W. H. *Chem. Mater.* **1999**, *11*, 2493−2500.
(46) Yang, C. S.; Kauzlarich, S. M.; Wang, Y. C. *Chem. Mater.* **1999**, *11*, 3666−3670.
(47) Yang, C.-S.; Kauzlarich, S. M.; Wang, Y. C. *Chem. Mater.* **1999**, *11*, 3666−3670.
(48) Yang, C. S.; Liu, Q.; Kauzlarich, S. M.; Phillips, B. *Chem. Mater.* **2000**, *12*, 983−988.
(49) Taylor, B. R.; Fox, G. A.; Hope-Weeks, L. J.; Maxwell, R. S.; Kauzlarich, S. M.; Lee, H. W. H. *Mater. Sci. Eng.* **2002**, *B96*, 90−93.

Different methods for terminating the nanoparticles were investigated. In many of the reactions, after the reflux step, the solvent was removed under reduced pressure and freshly distilled solvent was introduced along with the alkyl lithium reagent. However, this step appeared to be unnecessary for reactions that used stoichiometric amounts of bromine. For subsequent reactions, the termination step involved cooling the refluxed mixture to −50 °C and the addition of the terminating reagent to the mixture. For these two methods, no significant differences in the IR spectra or yields of the product could be observed. The use of hexane solvent in the termination step was also explored. In this case, freshly distilled hexane was added after removal of glyme solvent. The effects of changing the amount of added alkyl lithium reagent were also investigated. It was found that the use of excess *n*-butyl lithium resulted in higher yields of product. This was attributed to more complete termination or passivation of the nanoparticles. An investigation of the residue from the water rinse supported this conclusion. It was determined by microprobe analysis that the white solid resulting from drying the water extract was primarily $SiO_x$ along with the expected salt side products. In glyme, the reaction always produced a product with Si−O and Si−O−C stretches in the FTIR. To control the surface better, after the addition of *n*BuLi, and subsequent removal, dried *n*BuOH was added. The effect of solvent and termination methodology is further discussed in conjunction with the FTIR characterization (see below).

**Characterization.** *Transmission Electron Microscopy (TEM).* TEM, HRTEM, and EDX were used to establish and confirm the identity of the nanoparticles isolated from hexane. All of the reactions produced nanoparticles that showed similar micrographs of high faceted crystallites. In all cases, the lattice fringes are consistent with the diamond structure of silicon. Lattice fringes were measured from the negative micrograph and are consistent with the {111} planes (3.14 Å) of silicon and in some cases the {202} planes (1.92 Å). The diameter of the nanoparticles ranged from 1 to 20 nm with the majority in the range of 3−6 nm. To further ensure that the particles are composed of silicon, they were examined by EDX and silicon, carbon, and oxygen were observed. Some of the carbon and oxygen are attributed to the amorphous carbon grid. In addition to EDX, elemental mapping and energy-filtered images were obtained to illustrate the presence of silicon in the nanoparticles. Figure 2 shows an example of silicon mapping for some nanoparticles. Figure 2a shows a typical bright field image, (b) shows a silicon energy-filtered image, and (c) shows the difference mapping for silicon. To obtain a better understanding of how to obtain such a micrograph, visualize a silicon edge on an EELS spectrum. For the silicon map, one image is obtained using only the electrons in the energy range of 105−115 eV, which contains electrons from the silicon and the continuous background electrons. Two additional images were obtained using the electrons below the silicon edge, defining the slope of the background, which was then subtracted from the first image to leave only silicon intensity, Figure 2c. This figure shows that the particles are indeed silicon.

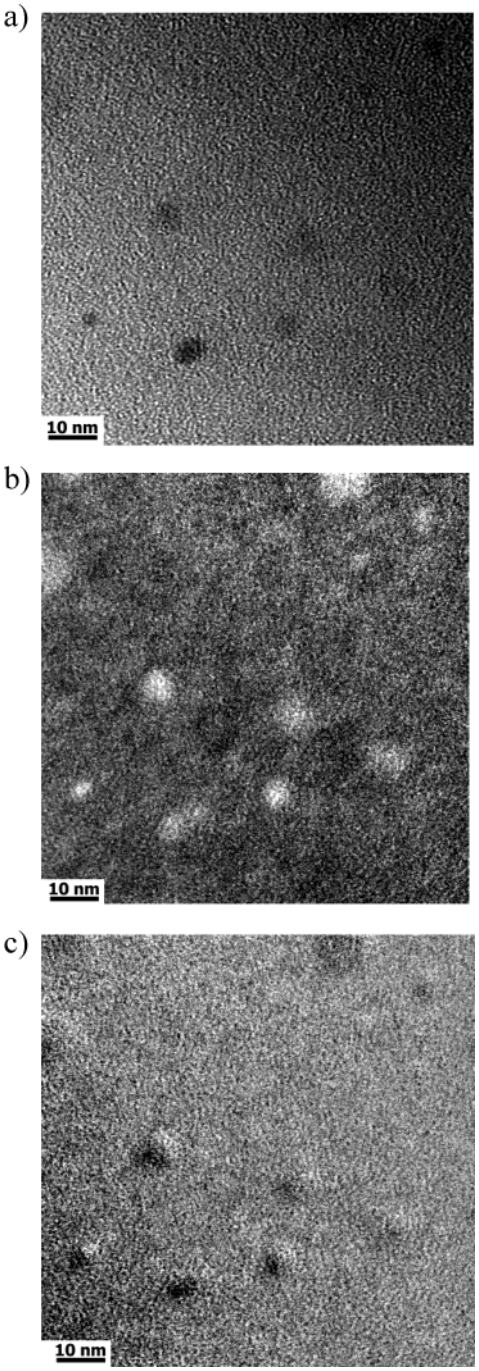


**Figure 2.** HRTEM micrographs of silicon mapping for silicon nanoparticles: (a) bright field micrograph, (b) micrograph with energy filtered to remove the silicon edge, and (c) silicon mapping micrograph.

A micrograph of the *n*-butyl-terminated silicon nanoparticles is shown in Figure 3. Both high resolution with lattice fringes and slightly lower magnification images are shown. These particles were obtained from a reaction with octane as the solvent. The nanoparticles appear to be of uniform size but there are large numbers of particles that are aggregated. Multiple images were obtained of the sample to obtain an adequate representation, and a histogram of the size distribution was constructed using approximately 300 nanoparticles. On the basis of the particles observed by HRTEM, the average diameter is 4.9 (2.3) nm. If only those nanoparticles below 10 nm are considered, the average

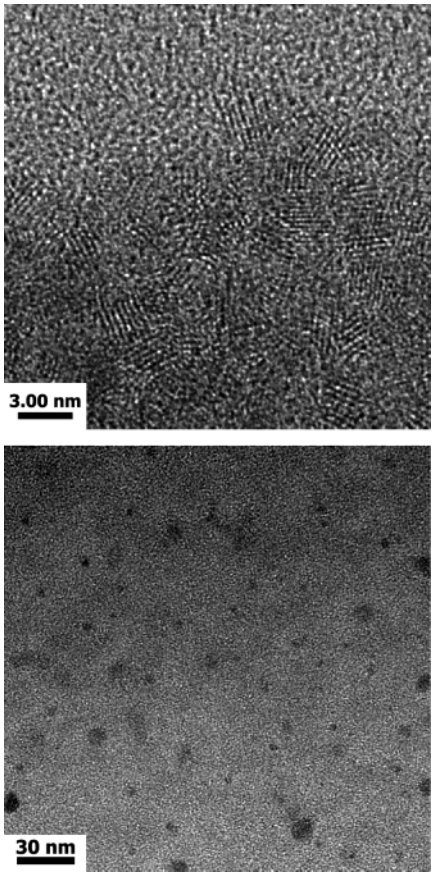


**Figure 3.** HRTEM micrographs of silicon nanoparticles prepared by oxidation in octane solvent and alkyl-capped. Top view shows particles with lattice fringes; bottom view shows a typical image for this sample.

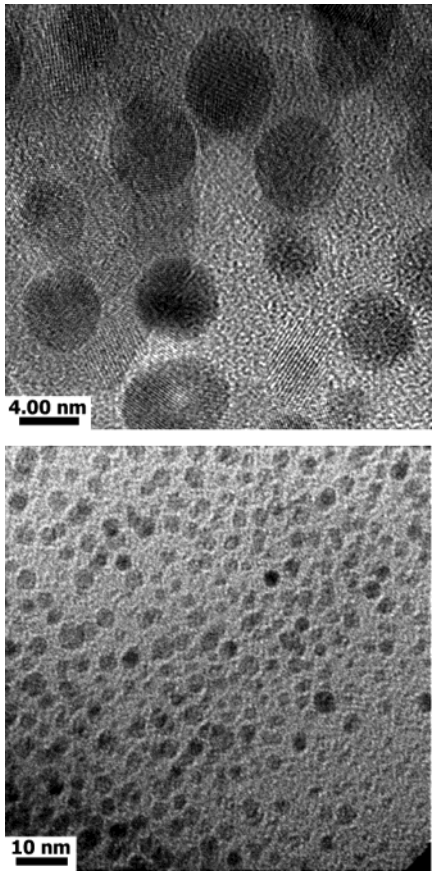


**Figure 4.** HRTEM micrographs of silicon nanoparticles prepared by oxidation in glyme solvent and alkyl-alkoxide-capped. Top view shows particles with lattice fringes; bottom view shows a typical image for this sample. The hexagonal shape of the nanocrystallites is clearly seen in the bottom view.

diameter is 4.8 (2.1) nm. Since sizes above 8 nm are not expected to contribute to the photoluminescence, the average diameter contributing to photoluminescence was determined to be 4.4 (1.7) nm.

A typical HRTEM image for silicon nanoparticles produced from the reaction in glyme, with the use of an alkyl lithium reagent for termination, is shown in Figure 4. The high-resolution image shows lattice fringes and the lower magnification image shows a large number of particles with facets. It can be seen that the nanoparticles are of fairly uniform size and clearly show lattice fringes corresponding to the {111} and {220} planes of crystalline silicon. The particles also appear well-faceted in the micrographs. A histogram was generated from the measurements of approximately 1000 nanoparticles. The yield of nanoparticles obtained from this reaction is almost 4 times larger than the reaction carried out in octane. The average diameter of the entire sample obtained from HRTEM is similar to that obtained from the reaction in octane, 4.8 (2.0) nm. For comparison, when the range 1−10 nm is used, the average diameter is determined to be 4.6 (1.7) nm. When the range 1−8 nm is used, the average diameter is 4.4 (1.5) nm, the same as the sample prepared from octane.

In either reaction, the nanoparticles produced that should show photoluminescence have an average size of about 4.4 (1.6) nm. Figures 3 and 4 are consistent with the best images from solution reactions and show considerable difference from HRTEM images from gas-phase pyrolysis[50−53] and other high-temperature methods.[54,55] The products from these low-temperature solution reactions tend to be highly faceted and show no amorphous surface that could be attributed to oxide. While it is difficult to prepare high-quality images of silicon, these images are comparable to our previously published work,[7,8,13,35] as well as to crystallites obtained from supercritical and high-pressure solution reactions.[4,9,11]

Attempts to obtain differently sized nanoparticles by changing the reflux time produced nanoparticles of similar size to those described above. Several reactions were performed to determine if the capping step affected the size of the nanoparticles. The length of time as well as the solvent used during the termination step was varied, but TEM indicated that this step had little to no effect on the size of the nanoparticles.

*Infrared Spectroscopy*. FTIR spectroscopy was used to identify and characterize the terminating moieties on the surface of the nanoparticles. Figure 5 shows the

(50) Littau, K. A.; Szajowshki, P. J.; Muller, A. J.; Kortan, A. R.; Brus, L. E. *J. Phys. Chem.* **1993**, *97*, 1224.
(51) Wilson, W. L.; Szajowski, P. F.; Brus, L. E. *Science* **1993**, *262*, 1242−1244.
(52) Brus, L. E.; Szajowski, P. F.; Wilson, W. L.; Harris, T. D.; Schuppler, S.; Citrin, P. H. *J. Am. Chem. Soc.* **1995**, *117*, 2915.
(53) Fojtik, A.; Weller, H.; Fiechter, S.; Henglein, A. *Chem. Phys. Lett.* **1987**, *134*, 477−479.
(54) Takagi, H.; Ogawa, H.; Yamazaki, Y.; Ishizaki, A.; Nakagiri, T. *Appl. Phys. Lett.* **1990**, *56*, 2379−2380.
(55) Saunders: W. A.; Sercel, P. C.; Lee, R. B.; Atwater, H. A. *Appl. Phys. Lett.* **1993**, *63*, 1549−1551.

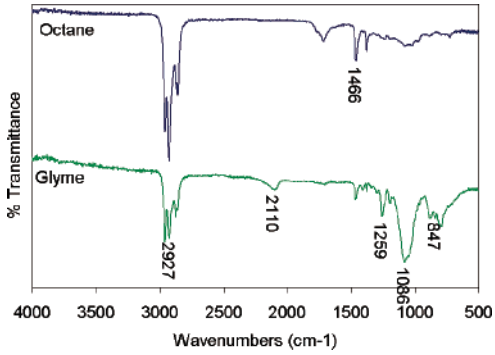


**Figure 5.** FTIR spectra of silicon nanoparticles prepared from either octane or glyme as the solvent.

FTIR spectrum for the *n*-butyl-terminated silicon nanoparticles prepared in *n*-octane. The characteristic methylene and terminated methyl stretching modes, 2870−2955 $cm^{-1}$, indicated the presence of $-CH_2-$ and $-CH_3$ groups along with very little evidence of silicon−oxygen stretching, in the 1020−1080-$cm^{-1}$ region. The FTIR spectrum is similar to that previously reported for the metathesis route, which also showed little evidence for silicon−oxygen stretching bands.[7]

In all of the reactions that used glyme as a solvent there is always a silicon−oxygen stretching absorption present in the IR spectrum; however, the percentage of transmittance of this stretch is variable and ranged from weak to very strong. The silicon−oxygen stretching absorption could be due to either oxygen contamination to the sample or side products that were formed during the reaction and not separated from the product. It is possible that the bromine is a strong enough oxidant to attack the glyme solvent or the alkyl lithium reagent is attacking the ether solvent,[56] which then could bond to the silicon. It is therefore proposed that these nanoparticles have both alkyl and alkoxy termination on the surface. The sample prepared in glyme was then purposefully terminated first with *n*BuLi and then with *n*BuOH. Figure 5 shows the FTIR spectrum for the *n*-butyl-terminated silicon nanoparticles prepared in glyme with use of an alkyl-lithium reagent and *n*BuOH for termination. The FTIR spectrum is similar to that reported for silicon nanoparticles prepared in supercritical octanol[9] with the notable absence of a hydroxyl stretch at 3360 $cm^{-1}$ and the presence of a double absorption corresponding to the Si−O−C linkage at 1070−1100 $cm^{-1}$. In addition, the presence of Si−H stretch at 2102 $cm^{-1}$ is noted. Detailed studies[41] of the use of alkyl lithium reagents on flat silicon surfaces suggest LiH is a byproduct that may attack the surface further, resulting in a lithium ion association to the silicon.[57] For this reason a slightly acidic rinse was used in the separation process, to replace any lithium sites with hydrogen.

*Optical Properties.* Figure 6 shows the UV−vis spectra of the two different samples, the alkyl- and the alkyl/alkoxy-terminated sample, dissolved in hexane. They show different room-temperature absorbances. The samples are the same average size, based on TEM; however, their size distributions and surface terminations are different. The product of the reaction in octane shows the more blue-shifted absorbance. These nanoparticles are apparently all alkyl-capped, based on the absence of the Si−O stretch in the FTIR spectrum. The product from the reaction in glyme shows a red-shifted absorbance. The nanoparticles prepared from the reaction in glyme are both alkyl- and alkoxy-capped, according to the FTIR spectrum. This is the first evidence that silicon nanoparticles of the same average size can afford different absorptions. While the exact shift differs from sample to sample, depending on synthesis, samples which show Si−O stretches in the FTIR are consistently red-shifted from samples which do not show Si−O stretches. The photoluminescence excitation (PLE) and emission (PL) spectra for the two differently terminated samples in hexane are illustrated in Figure 7. There is no detectable emission observed in the spectra above 600 nm in either case. Photoluminescence spectra were measured at room temperature and the emission spectra were collected with excitation wavelengths ranging from 250 to 450 nm as shown in Figure 8. The monotonic shift of the PL as a function of excitation wavelength results from the excitation of different sizes of nanocrystals that have different optical transition energies, thus confirm-

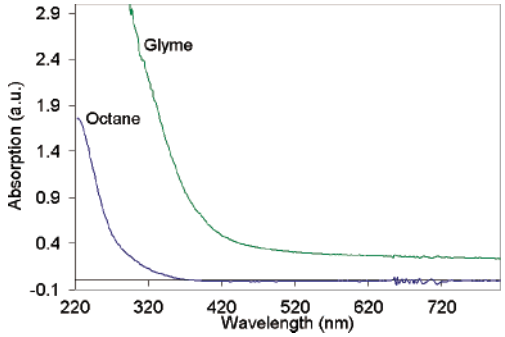


**Figure 6.** UV−visible spectra of silicon nanoparticles, recorded for the colloids in hexane.

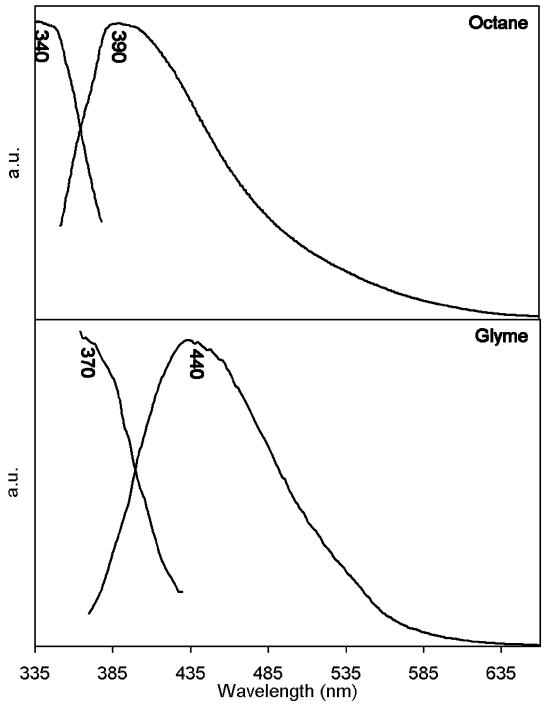


**Figure 7.** Max. PLE and PL of silicon nanoparticles for the samples prepared from either octane or glyme as the solvent.

(56) Coates, G. E.; Green, M. L. H.; Powell, P.; Wade, K. *Principles of Organometallic Chemistry*; Methuen & Co Ltd: London, 1968.
(57) Song, J. H.; Sailor, M. J. *Inorg. Chem.* **1999**, *38*, 1498−1503.

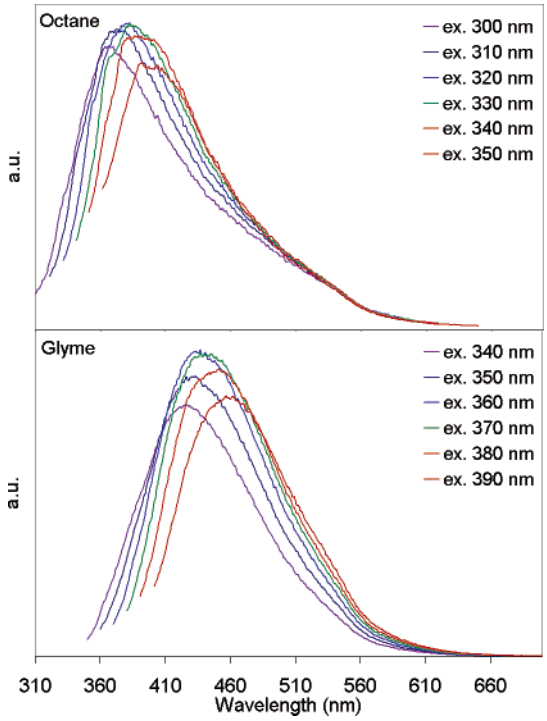


**Figure 8.** PL of silicon nanoparticles for the samples prepared from either octane or glyme as the solvent.

ing size-dependent energy levels consistent with a quantum confinement model. The size distribution is evident from the emission of the sample over a range of energies in the visible region.

The spectra in Figures 7 and 8 are consistent with a size distribution for both samples. The highest intensity emission spectrum for the alkyl-terminated nanoparticles is centered at 383 nm. The emission spectra for the alkyl/alkoxy-terminated nanoparticles were collected with excitation wavelengths that ranged from 340 to 390 nm in 10-nm increments, with the highest intensity emission spectrum centered at 440 nm. The PL is remarkably stable and these samples did not degrade in the presence of air over a period of about 1 year.

The PL maxima for the samples terminated with the alkyl lithium reagent are comparable to those of the smaller size hydrogen-terminated nanoparticles and alkoxide-terminated nanoparticles published by other groups.[5,9] The PL spectra of the nanoparticles in octane showed fairly broad full-widths at half-maximum (fwhm) absorbances, 80−97 nm (0.66−0.61 eV). These fwhm absorbances are similar in energy to those reported for 2-nm-diameter, hydrogen-terminated, silicon nanoparticles[5] and 1.5-nm-diameter alkoxy-terminated nanoparticles.[9] The samples reported here contain a distribution of sizes and it is probable that the smallest sizes dominate the photoluminescence spectra. Silicon nanoparticles remain indirect band gap semiconductors even at the smallest sizes,[15] and since the oscillator strength depends on size, the photoluminescence of the smaller quantum dots are expected to be significantly greater than the larger ones. In addition, since the size distribution is based on HRTEM images, the average size provided is biased toward the larger sizes. However, the average sizes and relative numbers of particles of the different sizes appear to be the same for the alkyl- and alkyl/alkoxy-terminated samples described herein, so the photoluminescence can be compared. The nanoparticles from both reactions have the same average diameter (4.4 nm), and their maximum PL emissions differ by 55 nm (0.41 eV). The particles were prepared in a similar manner, so differences in the photoluminescence may be contributing to differences in the surface termination and resulting surface defects. The effects of different passivants on silicon nanoparticles up to 2 nm in diameter have been performed using density functional theory (DFT) and quantum Monte Carlo (QMC).[30,32,33] The effect of changing a single hydrogen with a single −OH group produces a slightly smaller band edge, consistent with our experimental findings. The direction and the small size of the shift in emission observed with these samples, which have similar average size, suggests that the surface termination and resulting defects are responsible for the difference.

**Acknowledgment.** We thank Chris Nelson for help with the EDS and Valerie Leppert for useful discussion. This work was supported by the NSF (DMR-9803074, 0120990). K.A.P. received support from an NSF IGERT "Nanomaterials in the Environment, Agriculture and Technology". Work at the National Center for Electron Microscopy (NCEM) was performed under the auspices of the Director, Office of Energy Research, Office of Basic Energy Science, Materials Science Division, U.S. Department of Energy under Contract DE-Ac-03-76XF00098.

CM034403K